An Error Estimation and Mesh Refinement Method Applied to Optimal Libration Point Orbit Transfers

George V. Haman III¹ and Anil V. Rao²

Abstract—An adaptive mesh refinement method for numerically solving optimal control problems is described. The method employs collocation at the Legendre-Gauss-Radau points. Within each mesh interval, a relative error estimate is derived based on the difference between the Lagrange polynomial approximation of the state and an adaptive forward-backward explicit integration of the state dynamics. Accuracy in the method is achieved by adjusting the number of mesh intervals and degree of the approximating polynomial in each mesh interval. The method is demonstrated on time-optimal transfers from an L_1 halo orbit to an L_2 halo orbit in the Earth-Moon system, and performance is compared against previously developed mesh refinement methods.

I. INTRODUCTION

Over the past decade, hp-adaptive direct collocation methods for solving optimal control problems have gained significant attention due to their robustness and ability to outperform h and p methods in terms of computational efficiency and mesh size reduction. In an hp-adaptive direct collocation method, the domain of the optimal control problem is partitioned into intervals, and state approximations are applied in each interval at a specific set of support, i.e., *collocation*, points. As a result, the continuous-time optimal control problem is transcribed into a large, sparse, finite-dimensional nonlinear programming (NLP) problem, which can then be solved using well-developed software [1].

A *local* collocation method typically takes the form of an h method, where the degrees of the state approximations are fixed and constant across all intervals; however, the number of intervals can vary. As a result, convergence of an h method is achieved by increasing the number and/or placement of mesh points [2]. A global collocation method typically takes the form of a p method, where the number of intervals is fixed; however, the degrees of the state approximations can vary across intervals. Obtaining high-accuracy solutions using a p method may require an unreasonably high-degree polynomial approximation [3]. To gain maximum effectiveness, p methods have been developed using Gaussian quadrature collocation (GQC) [3]-[7], which employ collocation at the Legendre-Gauss (LG) [4], Legendre-Gauss-Radau (LGR) [5]-[7], or Legendre-Gauss-Lobatto (LGL) [3] points. When the optimal control problem solution takes on a smooth form, GQC methods are capable of converging to highly accurate solutions at an exponential rate [8]. In hp-adaptive methods, the number of intervals h and approximating polynomial degree p in each interval are both allowed to vary. These methods often adjust the number of mesh intervals in regions where the solution is non-smooth and/or adjust the degree of the polynomial in intervals where the solution is smooth. Such hp-adaptive methods can obtain similar accuracy to h methods on a smaller mesh and achieve convergence where p methods cannot.

Several adaptive direct GQC methods have been developed [9]-[13]. Ref. [9] uses convergence rates of the LGR collocation method and higher-order state derivatives to guide the hp refinement process, while detecting discontinuities in the control and reducing the size of the mesh when possible. The LGR collocation method utilized in Ref. [10] performs hp refinement based on the decay rate of the coefficients of a Legendre polynomial approximation of the state. Ref. [11] derives a relative error estimate, which is used in Refs. [9], [10], based on the difference between the Lagrange polynomial approximation of the state and an LGR quadrature integration of the dynamics in each interval to conduct p then h refinement. The h-adaptive LG and LGL collocation methods utilized in Refs. [12] and [13], respectively, obtain an error estimate between the Lagrange polynomial approximation of the state and an explicit propagation of the dynamics in each interval, and the corresponding mesh refinement techniques are applied to optimal libration point orbit transfers in the Earth-Moon circular restricted three-body problem (CR3BP). A closedform, analytical solution does not exist for many complex dynamical models, e.g., the CR3BP; therefore, numerical integration methods are required to propagate the system dynamics. Although h-adaptive LG and LGL collocation, i.e., implicit simulation, methods have been verified via explicit simulation, e.g., time-marching, schemes, this research presents a novel LGR quadrature collocation method employing an explicit hp mesh refinement technique.

The method developed in this paper extends the general mesh refinement ideas of Refs. [12], [13] to an hp-adaptive LGR quadrature collocation method. In this research, a relative error estimate is derived based on the difference between the Lagrange polynomial approximation of the state and an adaptive forward-backward explicit integration of the state dynamics at the LGR collocation points within each mesh interval. The method presented here employs the classical 4th-order Runge-Kutta (RK4) scheme and MATLAB's ode113 solver. Accuracy in the method is then achieved by adjusting the number of mesh intervals and/or degree of the

¹George V. Haman III, Ph.D. Candidate, Department of Mechanical and Aerospace Engineering, University of Florida, Gainesville, FL 32611, USA georgehaman@ufl.edu

²Anil V. Rao, Professor, Department of Mechanical and Aerospace Engineering, University of Florida, Gainesville, FL 32611, USA anilvrao@ufl.edu

approximating polynomial in each mesh interval. Finally, the method is demonstrated on time-optimal transfers from a 12-day L_1 halo orbit to a 15-day L_2 halo orbit in the Earth-Moon system, and performance is compared against the previously developed mesh refinement methods of Refs. [9]–[11].

II. BOLZA OPTIMAL CONTROL PROBLEM

Without loss of generality, consider the following *hp*-adaptive discretization of a continuous-time optimal control problem in Bolza form. The domain $\tau \in [-1, +1]$ is partitioned into a mesh consisting of K mesh intervals $S_k = [T_{k-1}, T_k] \subseteq [-1, +1], k = \{1, \ldots, K\}$, that satisfy

$$\bigcup_{k=1}^{K} \mathcal{S}_k = [-1, +1], \quad \bigcap_{k=1}^{K} \mathcal{S}_k = \{T_1, \dots, T_{K-1}\}, \quad (1)$$

where the mesh points are $-1 = T_0 < \cdots < T_K = +1$. The goal is to determine the state $\mathbf{x}^{(k)}(\tau) \in \mathbb{R}^{n_x}$ and control $\mathbf{u}^{(k)}(\tau) \in \mathbb{R}^{n_u}$ in mesh interval \mathcal{S}_k , $k = \{1, \ldots, K\}$, on the domain $\tau \in [-1, +1]$, initial time $t_0 \in \mathbb{R}$, and terminal time $t_f \in \mathbb{R}$ that minimize the objective functional

$$\mathcal{J} = \Phi[\mathbf{x}^{(1)}(-1), t_0, \mathbf{x}^{(K)}(+1), t_f]$$

$$+ \alpha \sum_{k=1}^{K} \int_{T_{k-1}}^{T_k} \mathcal{L}[\mathbf{x}^{(k)}(\tau), \mathbf{u}^{(k)}(\tau), t(\tau, t_0, t_f)] d\tau, \quad (2)$$

where $\alpha \equiv (t_f - t_0)/2$, subject to the dynamic constraints

$$d\mathbf{x}^{(k)}(\tau)/d\tau = \alpha \mathbf{f}[\mathbf{x}^{(k)}(\tau), \mathbf{u}^{(k)}(\tau), t(\tau, t_0, t_f)], \quad (3)$$

 $k = \{1, \dots, K\}$, the inequality path constraints

$$\mathbf{c}_{\min} \le \mathbf{c}[\mathbf{x}^{(k)}(\tau), \mathbf{u}^{(k)}(\tau), t(\tau, t_0, t_f)] \le \mathbf{c}_{\max}, \quad (4)$$

 $k = \{1, \dots, K\}$, the boundary conditions

$$\mathbf{b}_{\min} \le \mathbf{b}[\mathbf{x}^{(1)}(-1), t_0, \mathbf{x}^{(K)}(+1), t_f] \le \mathbf{b}_{\max},$$
 (5)

and the state continuity conditions $\mathbf{x}^{(k)}(T_k) = \mathbf{x}^{(k+1)}(T_k)$, $k = \{1, \dots, K-1\}$. Note that continuity of the control at the interior mesh points is not enforced.

III. LEGENDRE-GAUSS-RADAU COLLOCATION

The multiple-interval formulation of the continuous-time Bolza optimal control problem in Section II is discretized using collocation at the standard LGR points [5]–[7]. In the LGR quadrature collocation method, the state in mesh interval S_k , $k = \{1, \ldots, K\}$, is approximated as

$$\mathbf{x}^{(k)}(\tau) \approx \mathbf{X}^{(k)}(\tau) = \sum_{j=1}^{N_k+1} \mathbf{X}_j^{(k)} \ell_j^{(k)}(\tau), \tag{6}$$

where $\tau\in[-1,+1],$ $\ell_j^{(k)}(\tau),$ $j=\{1,\ldots,N_k+1\},$ is a basis of Lagrange polynomials given by

$$\ell_j^{(k)}(\tau) = \prod_{\substack{l=1\\l \neq j}}^{N_k+1} \frac{\tau - \tau_l^{(k)}}{\tau_j^{(k)} - \tau_l^{(k)}},\tag{7}$$

 $au_1^{(k)},\dots, au_{N_k}^{(k)}$ are the standard LGR collocation points in $\mathcal{S}_k=[T_{k-1},T_k)$, and $au_{N_k+1}^{(k)}=T_k$ is a noncollocated point.

The objective functional of Eq. (2) is approximated using a Gauss-Radau quadrature as

$$\mathcal{J} \approx \Phi[\mathbf{X}_{1}^{(1)}, t_{0}, \mathbf{X}_{N_{K}+1}^{(K)}, t_{f}] + \alpha \sum_{k=1}^{K} \sum_{i=1}^{N_{k}} w_{i}^{(k)} \mathcal{L}[\mathbf{X}_{i}^{(k)}, \mathbf{U}_{i}^{(k)}, t(\tau_{i}^{(k)}, t_{0}, t_{f})], \quad (8)$$

where $\mathbf{X}_1^{(1)}$ and $\mathbf{X}_{N_K+1}^{(K)}$ are the approximations of $\mathbf{x}(T_0)$ and $\mathbf{x}(T_K)$, respectively. In mesh interval \mathcal{S}_k , $k=\{1,\ldots,K\}$, $w_i^{(k)}$ and $\mathbf{U}_i^{(k)}$, $i=\{1,\ldots,N_k\}$, are the LGR quadrature weights and control approximations at the N_k LGR points, respectively. Differentiating $\mathbf{X}^{(k)}(\tau)$ in Eq. (6) with respect to τ yields

$$\frac{d\mathbf{x}^{(k)}(\tau)}{d\tau} \approx \frac{d\mathbf{X}^{(k)}(\tau)}{d\tau} = \sum_{j=1}^{N_k+1} \mathbf{X}_j^{(k)} \frac{d\ell_j^{(k)}(\tau)}{d\tau}.$$
 (9)

Collocating the dynamic constraints of Eq. (3) at the N_k LGR points in mesh interval S_k , $k = \{1, ..., K\}$, using Eq. (9) yields the defect constraints as

$$\sum_{j=1}^{N_k+1} D_{ij}^{(k)} \mathbf{X}_j^{(k)} - \alpha \mathbf{f}[\mathbf{X}_i^{(k)}, \mathbf{U}_i^{(k)}, t(\tau_i^{(k)}, t_0, t_f)] = \mathbf{0}, \quad (10)$$

 $i=\{1,\ldots,N_k\}$, where the elements of the LGR differentiation matrix are $D_{ij}^{(k)}\equiv \mathrm{d}\ell_j^{(k)}(\tau_i^{(k)})/\mathrm{d}\tau,\ i=\{1,\ldots,N_k\},\ j=\{1,\ldots,N_k+1\}.$ The inequality path constraints of Eq. (4) are enforced at the N_k LGR points in mesh interval $\mathcal{S}_k,\ k=\{1,\ldots,K\}$, as

$$\mathbf{c}_{\min} \le \mathbf{c}[\mathbf{X}_{i}^{(k)}, \mathbf{U}_{i}^{(k)}, t(\tau_{i}^{(k)}, t_{0}, t_{f})] \le \mathbf{c}_{\max},$$
 (11)

 $i=\{1,\ldots,N_k\}$. The boundary conditions of Eq. (5) are approximated at the endpoints as

$$\mathbf{b}_{\min} \le \mathbf{b}[\mathbf{X}_1^{(1)}, t_0, \mathbf{X}_{N_K+1}^{(K)}, t_f] \le \mathbf{b}_{\max}.$$
 (12)

The state continuity conditions are explicitly enforced via $\mathbf{X}_{N_k+1}^{(k)} = \mathbf{X}_1^{(k+1)}$, $k = \{1, \dots, K-1\}$, by treating $\mathbf{X}_{N_k+1}^{(k)}$ and $\mathbf{X}_1^{(k+1)}$ as the same variable. The resulting NLP problem is stated as follows. Minimize the cost function of Eq. (8) subject to the constraints of Eqs. (10)–(12).

IV. ADAPTIVE MESH REFINEMENT METHOD

The laws governing motion in a given dynamical model are represented by a set of differential equations. Because every optimal control problem is associated with a set of dynamic constraints, numerical integration methods for solving these differential equations are required in order to obtain solutions to optimal control problems numerically. These numerical integration techniques can be categorized as either explicit or implicit simulation methods, which are both equally valid; therefore, the adaptive mesh refinement method developed here seeks to validate the implicit simulation technique, i.e., collocation, utilized in Section III via an explicit simulation technique, e.g., time-marching. Based on the maximum relative error in the state determined via the implicit and explicit simulation methods, the mesh is refined until a desired mesh tolerance ε is satisfied.

A. Adaptive Explicit Simulation

An explicit simulation method solves the set of differential equations in the form of the initial value problem (IVP)

$$\dot{\mathbf{x}}(t) = \mathbf{f}[\mathbf{x}(t), \mathbf{u}(t), t]. \tag{13}$$

Consider the closed time interval $t \in [t_i, t_{i+1}], t_{i+1} > t_i$, over which is it desired to solve Eq. (13). Integrating Eq. (13) forward from the initial condition $\mathbf{x}(t_i) \equiv \mathbf{x}_i$ provides the value of the state $\mathbf{x}_{i+1} \equiv \mathbf{x}(t_{i+1})$ at any time $t_{i+1} > t_i$. Integrating Eq. (13) backward from the terminal condition $\mathbf{x}(t_{i+1}) \equiv \mathbf{x}_{i+1}$ provides the value of the state $\mathbf{x}_i \equiv \mathbf{x}(t_i)$ at any time $t_i < t_{i+1}$. Any numerical integration method can be used to perform the forward and backward steps; however, performance of the method presented in this research will depend on the numerical integration scheme chosen.

Now suppose that the NLP problem of Eqs. (8) and (10)–(12) corresponding to the discretized optimal control problem is solved on mesh \mathcal{M} with N_k LGR points in mesh interval $\mathcal{S}_k = [T_{k-1}, T_k], \ k = \{1, \dots, K\}$. Let the adaptive explicit simulation scheme yield values of the state $\hat{\mathbf{X}}^{(k)}(\hat{\tau}_1^{(k)}), \dots, \hat{\mathbf{X}}^{(k)}(\hat{\tau}_{P_k}^{(k)})$ at the points $\hat{\tau}_1^{(k)}, \dots, \hat{\tau}_{P_k}^{(k)}$, respectively, in mesh interval \mathcal{S}_k , $k = \{1, \dots, K\}$, where $\{\tau_1^{(k)}, \dots, \tau_{N_k+1}^{(k)}\} \subseteq \{\hat{\tau}_1^{(k)}, \dots, \hat{\tau}_{P_k}^{(k)}\}, \hat{\tau}_1^{(k)} = \tau_1^{(k)} = T_{k-1},$ and $\hat{\tau}_{P_k}^{(k)} = \tau_{N_k+1}^{(k)} = T_k$. Furthermore, let the values of the state approximation given in Eq. (6) at the collocation points $\tau_1^{(k)}, \dots, \tau_{N_k}^{(k)}$ and noncollocated point $\tau_{N_k+1}^{(k)}$ be denoted $\mathbf{X}^{(k)}(\tau_1^{(k)}), \dots, \mathbf{X}^{(k)}(\tau_{N_k}^{(k)})$ and $\mathbf{X}^{(k)}(\tau_{N_k+1}^{(k)})$, respectively. Note that for the IVP in Eq. (13), the initial condition $\hat{\mathbf{X}}^{(k)}(\hat{\tau}_1^{(k)}) = \mathbf{X}^{(k)}(\tau_1^{(k)})$ is used for forward integration, and the terminal condition $\hat{\mathbf{X}}^{(k)}(\hat{\tau}_{P_k}^{(k)}) = \mathbf{X}^{(k)}(\tau_{N_k+1}^{(k)})$ is used for backward integration. The points $\hat{\tau}_l^{(k)}$, $l = \{1, \dots, P_k\}$, are not all necessarily collocation points, e.g., an RK4 step requires function evaluations at the interval midpoint; therefore, a control interpolant must be defined. Let the control in mesh interval \mathcal{S}_k , $k = \{1, \dots, K\}$, be approximated as

$$\mathbf{U}^{(k)}(\tau) = \sum_{i=1}^{N_k} \mathbf{U}_j^{(k)} \hat{\ell}_j^{(k)}(\tau), \tag{14}$$

where $\tau \in [-1, +1]$, $\hat{\ell}_j^{(k)}(\tau)$, $j = \{1, \dots, N_k\}$, is a basis of Lagrange polynomials given by

$$\hat{\ell}_j^{(k)}(\tau) = \prod_{\substack{l=1\\l\neq j}}^{N_k} \frac{\tau - \tau_l^{(k)}}{\tau_j^{(k)} - \tau_l^{(k)}},\tag{15}$$

and $\tau_1^{(k)}, \ldots, \tau_{N_k}^{(k)}$ are the standard LGR collocation points in $\mathcal{S}_k = [T_{k-1}, T_k)$. The control interpolant in Eq. (14) can then be utilized at any point $\hat{\tau}^{(k)} \in [\hat{\tau}_1^{(k)}, \hat{\tau}_{P_k}^{(k)}]$, in mesh interval \mathcal{S}_k , $k = \{1, \ldots, K\}$.

B. Error Estimate in Mesh Interval

In mesh interval S_k , $k = \{1, ..., K\}$, let $\hat{\mathbf{X}}_{\pm}^{(k)}(\tau_l^{(k)})$, $l = \{1, ..., N_k + 1\}$, denote approximated values of the state obtained in Section IV-A via forward and backward integration, respectively. Then, the absolute and relative

errors in the i^{th} component of the state in mesh interval S_k , $k = \{1, \dots, K\}$, are defined, respectively, as

$$E_{i,\pm}^{(k)}(\tau_l^{(k)}) = \left| \hat{X}_{i,\pm}^{(k)}(\tau_l^{(k)}) - X_i^{(k)}(\tau_l^{(k)}) \right|, \tag{16}$$

$$e_i^{(k)}(\tau_l^{(k)}) = \frac{\max\left[E_{i,+}^{(k)}(\tau_l^{(k)}), E_{i,-}^{(k)}(\tau_l^{(k)})\right]}{1 + \max_{\substack{j \in \{1, \dots, N_k + 1\}\\k \in \{1, \dots, K\}}} \left|X_i^{(k)}(\tau_j^{(k)})\right|}, \tag{17}$$

 $i=\{1,\ldots,n_x\}$. Using Eq. (16), note that $E_{i,+}^{(k)}(\tau_1^{(k)})=0$ and $E_{i,-}^{(k)}(\tau_{N_k+1}^{(k)})=0$, $i=\{1,\ldots,n_x\},\ k=\{1,\ldots,K\}$, from the initial and terminal conditions provided for the IVP in Eq. (13), respectively. Then, the maximum relative error in mesh interval \mathcal{S}_k , $k=\{1,\ldots,K\}$, is defined as

$$e_{\max}^{(k)} = \max_{\substack{i \in \{1, \dots, n_x\}\\l \in \{1, \dots, N_k + 1\}}} e_i^{(k)}(\tau_l^{(k)}). \tag{18}$$

Although the explicit simulation scheme may require and/or use function evaluations at points other than the collocation points, only the relative state errors at the collocation points are considered. It is desired to meet the mesh tolerance ε , i.e., $e_{\max}^{(k)} \leq \varepsilon$, in every mesh interval \mathcal{S}_k , $k = \{1, \ldots, K\}$. If the mesh tolerance ε is not met in at least one mesh interval, then the current mesh is refined by dividing the appropriate mesh interval(s) into sub-intervals or increasing the degree of the approximating polynomial within the mesh interval(s).

C. Adjustment of Polynomial Degree in Mesh Interval

Suppose the maximum relative error $e_{\max}^{(k)}$ in Eq. (18) in a mesh interval \mathcal{S}_k , $k \in \{1, \dots, K\}$, exceeds the desired mesh tolerance ε , then the degree of the approximating polynomial, i.e., number of collocation points, in mesh interval \mathcal{S}_k is adjusted. To reduce the maximum relative error, the number of collocation points N_k in the appropriate mesh interval \mathcal{S}_k is strictly increased to

$$N_k^{\mathcal{M}+1} = N_k^{\mathcal{M}} + \left[\log_{10} \left(e_{\text{max}}^{(k)} / \varepsilon \right) \right], \tag{19}$$

where \mathcal{M} denotes the mesh iteration, and $\lceil \cdot \rceil$ replaces the argument with the next highest integer.

D. Adjustment of Number of Mesh Intervals

Let user-defined values N_{\min} and N_{\max} denote the minimum and maximum allowable number of collocation points in a mesh interval, respectively, where $2 \leq N_{\min} \leq N_{\max}$. Again, consider a mesh interval \mathcal{S}_k , $k \in \{1,\ldots,K\}$, in which the maximum relative error $e_{\max}^{(k)}$ exceeds the mesh tolerance ε . After adjusting the polynomial degree per the method of Section IV-C, mesh interval \mathcal{S}_k is divided into sub-intervals only if $N_k^{\mathcal{M}+1} > N_{\max}$. For the division of a mesh interval, it is desired to keep $N_k^{\mathcal{M}+1}$ total collocation points, as set by Eq. (19), as well as employ N_{\min} collocation points in each newly created sub-interval. Then, the number of sub-intervals, \mathcal{H}_k , is determined by

$$\mathcal{H}_k = \max(\left\lceil N_k^{\mathcal{M}+1}/N_{\min} \right\rceil, 2). \tag{20}$$

As a result, the full range of allowable polynomial degree approximations can be used in the new mesh.

E. Mesh Refinement Strategy

A summary of the adaptive mesh refinement method is shown below, which requires user-specified parameters: an explicit simulation scheme, mesh tolerance ε , minimum and maximum allowable number of collocation points N_{\min} and N_{\max} , respectively, in a mesh interval, and maximum number of mesh refinement iterations \mathcal{M}_{\max} .

Mesh Refinement Technique

- 1) Supply initial mesh, and set $\mathcal{M} = 0$.
- 2) Solve NLP from Section III on mesh \mathcal{M} .
- 3) Compute maximum relative error $e_{\text{max}}^{(k)}$ for all mesh intervals using Eq. (18) of Section IV-B.
- 4) If $e_{\text{max}}^{(k)} \leq \varepsilon$ for all mesh intervals or $\mathcal{M} > \mathcal{M}_{\text{max}}$, then quit. Otherwise proceed to Step 5).
- 5) Modify all mesh intervals using the methods of Sections IV-C and IV-D for which $e_{\max}^{(k)} > \varepsilon$.
- 6) Set $\mathcal{M} = \mathcal{M} + 1$, and return to Step 2).

V. CIRCULAR RESTRICTED THREE-BODY PROBLEM

In the CR3BP, the primary bodies move in circular orbits relative to the system's barycenter. The third body is assumed to have negligible mass compared to that of the primaries, i.e., $m_1 > m_2 \gg m$. To avoid numerical scaling issues, the CR3BP is nondimensionalized using the following quantities. The characteristic mass M is the sum of the masses of the primaries. The characteristic length \mathbb{L} is the distance between the primaries. The characteristic time $\mathbb T$ scales the characteristic gravitational constant \mathbb{G} to unity. The CR3BP equations of motion (EOMs) are commonly formulated in terms of a coordinate basis $\{\hat{\mathbf{x}}, \hat{\mathbf{y}}, \hat{\mathbf{z}}\}$ fixed in a uniformlyrotating reference frame, where \hat{x} points from the larger to smaller primary, $\hat{\mathbf{z}}$ is parallel to the primary system orbit's specific angular momentum vector, and $\hat{\mathbf{y}}$ is defined as the cross product of $\hat{\mathbf{z}}$ and $\hat{\mathbf{x}}$. Let $\rho(x,y,z) \equiv x\hat{\mathbf{x}} + y\hat{\mathbf{y}} + z\hat{\mathbf{z}}$ and $\hat{\mathbf{u}}(u_x, u_y, u_z) \equiv u_x \hat{\mathbf{x}} + u_y \hat{\mathbf{y}} + u_z \hat{\mathbf{z}}$ describe the position relative to the system's barycenter and unit control direction of the third body, respectively. To further assist in avoiding numerical difficulties with scaling, the third body's mass is transformed to $M \in [0,1]$ via $M(m) \equiv m/m_0$, where m_0 is the corresponding dimensionalized initial mass. Then, the controlled CR3BP EOMs can be written as

$$\ddot{\boldsymbol{\rho}} \equiv d^2 \boldsymbol{\rho} / dt^2 = [-2\hat{\mathbf{z}}]^{\times} \dot{\boldsymbol{\rho}} + \nabla_{\boldsymbol{\rho}} \mathcal{U} + \kappa T \hat{\mathbf{u}}, \qquad (21)$$

$$\dot{M} \equiv dM/dt = -\eta T,$$
 (22)

where $\kappa(M) \equiv \mathbb{T}^2/(\mathbb{L}Mm_0)$, $\eta \equiv \mathbb{T}/(m_0I_{\mathrm{sp}}g_0)$,

$$\mathcal{U}(x,y,z) \equiv (x^2 + y^2)/2 + (1-\mu)/r_1 + \mu/r_2, \quad (23)$$

$$r_1(x, y, z) \equiv [(x + \mu)^2 + y^2 + z^2]^{1/2},$$
 (24)

$$r_2(x, y, z) \equiv [(x - 1 + \mu)^2 + y^2 + z^2]^{1/2},$$
 (25)

and $\mu=m_2/\mathbb{M}$ is the system's mass ratio. Equation (22) accounts for any third body mass variation, where T is

the corresponding dimensionalized thrust magnitude. Two features of the uncontrolled CR3BP formulation are the admittance of an integral of motion and existence of five equilibrium points. The integral of motion, i.e., *Jacobi's constant*, is given by

$$C(x, y, z, \dot{x}, \dot{y}, \dot{z}) \equiv 2U - (\dot{x}^2 + \dot{y}^2 + \dot{z}^2),$$
 (26)

which serves as a useful tool for analyzing integration accuracy for any ballistic trajectory. The five equilibrium, i.e., Lagrange or libration, points are the real solutions to $\nabla_{\rho}\mathcal{U}|_{eq}=0$. Among the infinite periodic solutions existing in the CR3BP [14], such periodic solutions in the vicinity of the libration points are a prominent area of interest. Many libration point orbit families exist; however, this research only utilizes L_1 and L_2 northern halo orbits.

VI. MINIMUM-TIME ORBIT TRANSFER

A. Optimal Control Problem Formulation

The adaptive mesh refinement method described in Section IV is applied to time-optimal L_1 to L_2 halo orbit transfers in the Earth-Moon system. The optimal control problem is stated as follows. Minimize the objective functional

$$\mathcal{J} = t_f \tag{27}$$

subject to the constraints of Eqs. (21)-(22) and

$$\|\hat{\mathbf{u}}(t)\|^2 = 1, \quad r_{2,\min} \le r_2,$$
 (28)

$$\mathbf{x}(t_0) = \mathbf{x}_0, \quad \mathbf{x}(t_f) = \mathbf{x}_f. \tag{29}$$

The state and control are defined consistent with Section V as $\mathbf{x}(t) \equiv [x,y,z,\dot{x},\dot{y},\dot{z},M]$ and $\hat{\mathbf{u}}(t) \equiv [u_x,u_y,u_z]$, respectively. The path constraints of Eq. (28) ensure that the control direction is a unit vector and a minimum lunar distance is maintained. The boundary conditions of Eq. (29) ensure that the spacecraft departs from the 12-day L₁ halo orbit and arrives on the 15-day L₂ halo orbit prescribed by the Tab. I parameters from JPL's Three-Body Periodic Orbits toolbox. Note that $\mathcal{C}_0 \neq \mathcal{C}_f$; therefore, a ballistic transfer between the two orbits does not exist.

 $\label{eq:table I} \textbf{TABLE I}$ Initial L_1 and Terminal L_2 Halo Orbit Parameters

Parameter	Value	Units	
x_0	0.824293579889485	LU	
y_0	0	LU	
z_0	0.059984711782085	LU	
\dot{x}_0	$-7.040738167896908 \times 10^{-16}$	LU/TU	
\dot{y}_0	0.170850572731808	LU/TU	
\dot{z}_0	$-5.427041198051449 \times 10^{-15}$	LU/TU	
\mathcal{C}_0	3.145735258182749	LU ² /TU ²	
\mathcal{P}_0	12.253457628121380	days	
x_f	1.180836219582637	LU	
y_f	0	LU	
z_f	0.007995454197659	LU	
\dot{x}_f	$2.373346418664623 \times 10^{-15}$	LU/TU	
\dot{y}_f	-0.156226269091702	LU/TU	
$\dot{y}_f \ \dot{z}_f$	$2.247759466646941 \times 10^{-16}$	LU/TU	
\mathcal{C}_f	3.151838272450008	LU ² /TU ²	
\mathcal{P}_f	15.137550107547307	days	

For this investigation, the spacecraft's thrust magnitude is set to 0.5 N; other vehicle parameters include an initial

mass m_0 of 1000 kg and a thruster specific impulse $I_{\rm sp}$ of 3000 s. All results are obtained using the MATLAB general-purpose optimal control software $\mathbb{GPOPS}-\mathbb{II}$ [15]. The resulting NLP problem is solved using IPOPT [1] with a tolerance of $\varepsilon_{\rm NLP}=10^{-6}$. IPOPT is supplied first and second derivatives from a sparse central difference scheme. In addition, the hp-adaptive mesh refinement described in Section IV is employed using an explicit RK4 scheme and MATLAB's ode113 solver, $\varepsilon=10^{-6}$, $N_{\rm min}=2$, and $N_{\rm max}=10$ for all cases. Note that the RelTol and AbsTol options for ode113 are set to the mesh tolerance ε . As with many solvers, $\mathbb{GPOPS}-\mathbb{II}$ requires an initial guess, which is provided as a line connecting the initial and terminal states. The supplied initial mesh consists of 10 evenly spaced intervals with 4 collocation points in each interval.

Performance of the hp-adaptive mesh refinement described in this work is compared against the previously developed mesh refinement methods of Refs. [9]–[11], which are referred to as LR, LRL, and PR, respectively. These methods all utilize the same relative error estimate based on the difference between the Lagrange polynomial approximation of the state and an LGR quadrature integration of the dynamics in each interval, which is denoted $\tilde{e}_{\max}^{(k)}$, $k=\{1,\ldots,K\}$, as well as the same control interpolation method shown in Eq. (14). Then, let the following maximum relative errors over all intervals be

$$e_{\max} = \max_{k \in \{1, \dots, K\}} e_{\max}^{(k)}, \quad \tilde{e}_{\max} = \max_{k \in \{1, \dots, K\}} \tilde{e}_{\max}^{(k)}, \quad (30)$$

where $e_{\max}^{(k)}$ is obtained via Eq. (18).

B. Results and Discussion

Time-optimal L_1 to L_2 halo orbit transfers in the Earth-Moon system are obtained. Using the hp-adaptive method of Section IV with MATLAB's odel13 solver, the optimal transfer on the converged mesh is shown in Fig. 1. The corresponding position, velocity, and control components and mesh refinement history are shown in Figs. 2 and 3, respectively. As the hp-adaptive mesh refinement method described in Section IV iterates, collocation points are added in regions of rapid changes in the state, i.e., the density of the mesh increases when the spacecraft slingshots around the Moon, which occurs around t=1.1 TU in Fig. 2. Similar results were observed using an explicit RK4 scheme.

When analyzing performance, the objective values on the converged meshes and corresponding mesh size history, i.e., total number of collocation points in a given mesh, are shown in Tab. II. A optimal objective value, i.e., final time, of 2.129527 TU or 9.247428 days obtained via the method developed in this paper is consistent—within the specified NLP tolerance—with that obtained using previously developed methods, as shown in Tab. II.

As expected, the size of the mesh grows in order to satisfy the desired error tolerance. Although the RK4 method requires more mesh iterations than the PR method, it requires 205 fewer collocation points; a similar result is observed using ode113 with 213 fewer collocation points. The ode113

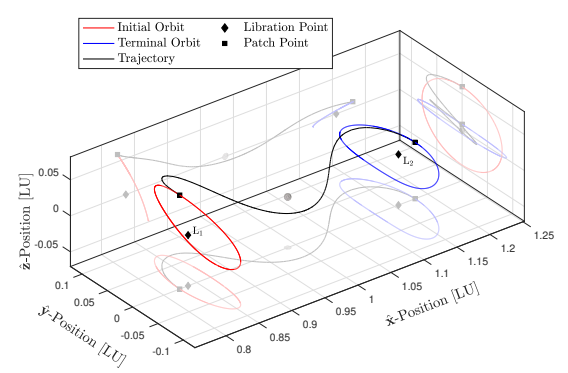


Fig. 1. Optimal libration point orbit transfer on converged mesh.

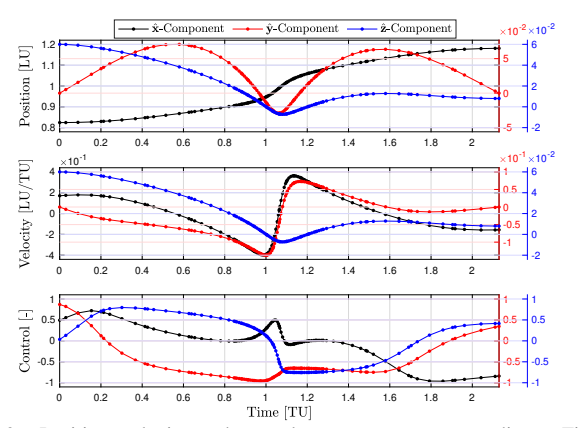


Fig. 2. Position, velocity, and control components corresponding to Fig. 1.

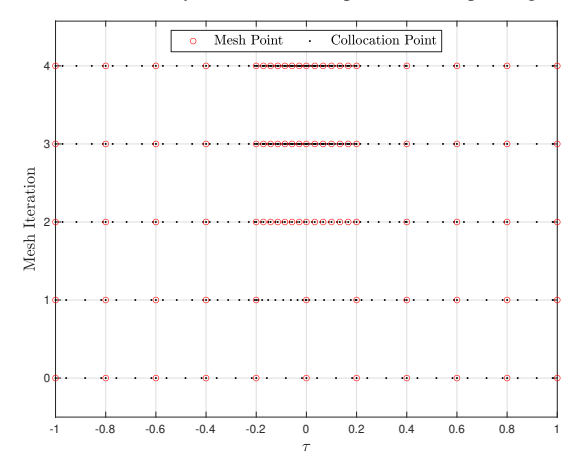


Fig. 3. Mesh refinement history corresponding to Fig. 1.

TABLE II
OBJECTIVE VALUE ON CONVERGED MESH AND MESH SIZE HISTORY

Method	Objective [TU]	Mesh Size on Refinement Iteration, M					
		1	2	3	4	5	6
RK4	2.1295270959	58	70	116	120	122	123
ode113	2.1295270957	57	69	113	115	-	-
PR	2.1295273539	67	193	328	-	-	-
LR	2.1295271290	58	72	98	105	-	-
LRL	2.1295271233	72	101	110	-	-	-

method converges in a similar number of iterations as the PR, LR, and LRL methods. A few more points are required when compared to the LR and LRL methods; however, the LR and LRL methods also employ schemes for reducing the size of the mesh, which are not implemented in the method presented in this work. Although the previously developed methods seem to outperform the method developed in Sec-

tion IV in terms of mesh size and/or computational efficiency, a discrepancy appears when analyzing convergence criteria. The corresponding maximum relative errors $e_{\rm max}$ and $\tilde{e}_{\rm max}$ on a given mesh $\mathcal M$ obtained via Eq. (30) are shown in Figs. 4 and 5, respectively. On the converged mesh for all methods discussed in this work, the condition $\tilde{e}_{\rm max} \leq \varepsilon$ is satisfied, as shown by Fig. 5; however, the condition $e_{\rm max} \leq \varepsilon$ is only satisfied on the converged mesh when using the currently developed method, as shown by Fig. 4. This premature convergence suggests that there is still some unaccounted for discrepancy between obtaining solutions via implicit and explicit simulation in the previously developed methods of Refs. [9]–[11]. The hp-adaptive mesh refinement method developed in this work, on the other hand, ensures consistency between the two simulation techniques.

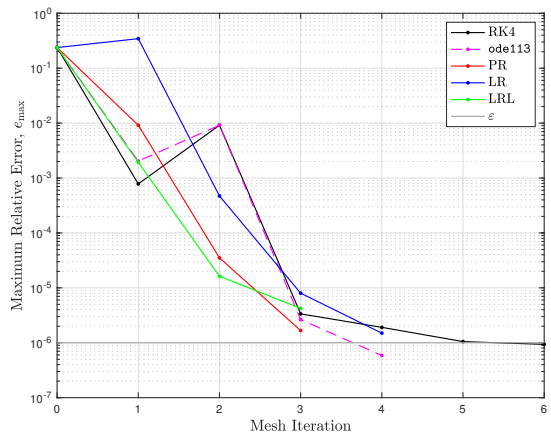


Fig. 4. Maximum relative error history for e_{max} .

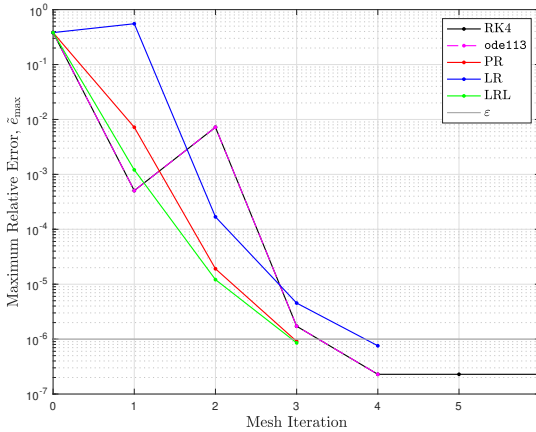


Fig. 5. Maximum relative error history for \tilde{e}_{max} .

VII. CONCLUSIONS

An adaptive mesh refinement method for solving optimal control problems using direct LGR collocation has been developed. The decision to adjust the number of mesh intervals and/or degree of the approximating polynomial within each interval is determined from a relative error estimate based on the difference between the Lagrange polynomial approximation of the state and an adaptive forward-backward explicit integration of the state dynamics. The method is then applied to time-optimal transfers between L₁ and L₂ halo orbits in the Earth-Moon system, and the corresponding results show that the approach outperforms a previously

developed *hp*-adaptive mesh refinement method in terms of final mesh size. The method presented in this research also ensures consistency between implicit and explicit simulation techniques, where previously developed *hp*-adaptive mesh refinement methods converge prematurely.

ACKNOWLEDGMENTS

The authors gratefully acknowledge support for this research from the U.S. National Science Foundation under grant CMMI-2031213 and the National Aeronautics and Space Administration (NASA) through the University of Central Florida's NASA Florida Space Grant and Space Florida under grant 80NSSC20M0093.

REFERENCES

- [1] L. T. Biegler and V. M. Zavala, "Large-Scale Nonlinear Programming Using IPOPT: An Integrating Framework for Enterprise-Wide Optimization," *Computers and Chemical Engineering*, vol. 33, no. 3, pp. 575–582, Mar. 2009.
- [2] J. T. Betts, Practical Methods for Optimal Control Using Nonlinear Programming, 3rd. Philadelphia, Pennsylvania: SIAM Press, 2010.
- [3] G. Elganar, M. A. Kazemi, and R. Razzaghi, "The Pseudospectral Legendre Method for Discretizing Optimal Control Problems," *IEEE Transactions on Automatic Control*, vol. 40, no. 10, pp. 1793–1796, Oct. 1995.
- [4] D. A. Benson, G. T. Huntington, T. P. Thorvaldsen, and A. V. Rao, "Direct Trajectory Optimization and Costate Estimation via an Orthogonal Collocation Method," *Journal of Guidance, Control, and Dynamics*, vol. 29, no. 6, pp. 1435–1440, Nov. 2006.
- [5] D. Garg, M. A. Patterson, C. L. Darby, et al., "Direct Trajectory Optimization and Costate Estimation of Finite-Horizon and Infinite-Horizon Optimal Control Problems Using a Radau Pseudospectral Method," Computational Optimization and Applications, vol. 49, no. 2, pp. 335–358, Jun. 2011.
- [6] D. Garg, M. A. Patterson, W. W. Hager, A. V. Rao, D. A. Benson, and C. T. Huntington, "A Unified Framework for the Numerical Solution of Optimal Control Problems Using Pseudospectral Methods," *Automatica*, vol. 46, no. 11, pp. 1843–1851, Nov. 2010.
- [7] D. Garg, W. W. Hager, and A. V. Rao, "Pseudospectral Methods for Solving Infinite-Horizon Optimal Control Problems," *Automatica*, vol. 47, no. 4, pp. 829–937, Apr. 2011.
- [8] W. W. Hager, J. Liu, S. Mohapatra, A. V. Rao, and X.-S. Wang, "Convergence Rate for a Radau hp Collocation Method Applied to Constrained Optimal Control," Computational Optimization and Applications, vol. 74, pp. 275–314, May 2019.
- [9] F. Liu, W. W. Hager, and A. V. Rao, "Adaptive Mesh Refinement Method for Optimal Control Using Nonsmoothness Detection and Mesh Size Reduction," *Journal of the Franklin Institute*, vol. 352, no. 10, pp. 4081–4106, Oct. 2015.
- [10] F. Liu, W. W. Hager, and A. V. Rao, "Adaptive Mesh Refinement Method for Optimal Control Using Decay Rates of Legendre Polynomial Coefficients," *IEEE Transactions on Control Systems Technology*, vol. 26, no. 4, pp. 1475–1483, Jul. 2018.
- [11] M. A. Patterson, A. V. Rao, and W. W. Hager, "A ph Mesh Refinement Method for Optimal Control," Optimal Control Applications and Methods, vol. 36, no. 4, pp. 398–4218, Jul. 2015.
- [12] R. E. Pritchett, K. C. Howell, and D. J. Grebow, "Low-Thrust Transfer Design Based on Collocation Techniques: Applications in the Restricted Three-Body Problem," in *Proceedings of the 2017 AAS/AIAA Astrodynamics Specialist Conference*, AAS Paper 17-626, Stevenson, Washington, Aug. 2017.
- [13] D. J. Grebow and T. J. Pavlak, "MColl: Monte Collocation Trajectory Design Tool," in *Proceedings of the 2017 AAS/AIAA Astrodynamics Specialist Conference*, AAS Paper 17-776, Stevenson, Washington, Aug. 2017.
- [14] V. G. Szebehely, Theory of Orbits: The Restricted Problem of Three Bodies. New York, New York: Academic Press, Inc., 1967.
- [15] M. A. Patterson and A. V. Rao, "GPOPS-II: A MATLAB Software for Solving Multiple-Phase Optimal Control Problems Using hp-Adaptive Gaussian Quadrature Collocation Methods and Sparse Nonlinear Programming," ACM Transactions on Mathematical Software, vol. 41, no. 1, Article 1:1–37, Oct. 2014.